

Wind Turbine Project Report

University of California, Berkeley
Mechanical Engineering Dept. E26

Project Team (Group 10):
*Eric Gu, Marwan Haggag, Steven Huynh,
Ivan Kuang, Kavish Kondap*

Professor Ken Youssefi
GSI Kate Gerhardt
December 13th, 2024



PROJECT SUMMARY

The objective of this Engineering 26 project was to design a blade rotor to optimize power output—when connected to a motor—and an accompanying wind turbine tower to maintain stiffness against applied loads. In addition to predefined constraints for weight, height, volume, and motor housing geometry, we considered the advantages and limitations of our fabrication method—FDM 3D printing—when designing each component.



Figure 1: Completed tower undergoing testing

During the onset of this project, we focused on the architecture of our rotor, beginning with an extensive literature review. Guided by the provided specifications, we attempted to select design parameters with the goal of maximizing power generation under a 25-mile-per-hour wind. Through research of related works from industry and academia, we found the following arguments to be critical to a rotor's efficiency: number of blades, angle of attack, blade profile, and twist angle. Beginning with hand-drawn models inspired by existing airfoil geometries, we soon refined a CAD model in Solidworks—while adhering to constraints on rotor diameter and hub geometry—which was later printed from ABS. During testing, our blade generated 0.5 watts of power at optimal resistance.

Similar to the rotor, our tower design began with structural design research during a lab session, followed by concept sketches to combine geometric principles with creative towers. After converting an initial concept to CAD, we underwent significant refinement through multiple design iterations, driven by feedback from finite element analysis simulations. Ultimately, this resulted in a design with a triangular base and spiraling truss upper half, providing our tower with a sturdy foundation and unique design. The tower was to be designed in two different parts to accommodate the 3D printer's size constraints (9x9x9 inches). The top half also includes the motor housing, with a 3/16 hole used to attach an eye bolt. During testing, we attached weights in 100g increments up to 1kg, resulting in a maximum deflection of 2.63mm. Our tower weighed 178 g with an empirical stiffness of 3.601N/mm. Ultimately, despite shortcomings, we successfully produced a tower that withstood the predefined load and a rotor that produced power under windy conditions.

TABLE OF CONTENTS

PROJECT SUMMARY.....	i
TABLE OF CONTENTS.....	ii
INTRODUCTION.....	1
DESIGN.....	5
Design Software:.....	5
Turbine Design:.....	6
Tower Design:.....	7
Finite Element Analysis:.....	9
TESTING AND RESULTS.....	11
Testing Procedure:.....	11
CAD DRAWINGS.....	18
CONCLUSIONS.....	21
RECOMMENDATIONS FOR FUTURE WORK.....	21
REFERENCES.....	22
APPENDICES.....	23

INTRODUCTION

Throughout history, humans have used technology to harvest the power of the wind. As early as 7000 years ago, humans realized they could use sails to capture wind energy to move their boats down the Nile River. 5000 years later, our species began using windmills to help with grinding grain. By the late 19th century, humans started using wind turbines that were able to convert the kinetic energy of the wind to usable electricity. While they were not initially very prevalent, their popularity spiked in the 1980s following a series of oil shortages. The share of energy produced by wind turbines has increased dramatically over the past few decades and continues to increase. In the United States, electricity generated from wind power has increased from 1% in 1990 to over 10% in 2022, with similar trends being observed across the globe.

One of the biggest reasons for this trend is that wind energy is much more sustainable than traditional energy generation methods, such as coal and fossil fuels. Using wind energy produces less pollution and harmful greenhouse gases such as carbon dioxide, which contribute to global warming. A 2022 report by the US Department of Energy found that wind energy helps prevent 336 million tons of carbon dioxide from being emitted annually. Converting our existing fossil fuel plants to cleaner techniques would only seek to benefit the environment and lessen the impact of global warming. Moreover, the efficiency—both in energy production and cost—of wind turbines leads to them being an appealing alternative. Wind farms, which include thousands of wind turbines, can collectively produce significant energy, thereby benefiting the economy, and reducing strain on the environment.

Through a macroscopic lens, wind turbines have three main components: the rotor, structure, and generator. When wind passes through a rotor, it induces a pressure differential, due to the airfoil geometry of each blade. This difference causes a lift, which overcomes the drag of spinning through the air, leading to rotational kinetic energy. Using a generator, this movement is converted into electrical energy.

In the status quo, there exist two designs for wind turbines: Horizontal Axis and Vertical Axis. Horizontal Axis Wind Turbines (HAWTs) are named as such because their rotor spins on an axis parallel to the wind. As the turbine directly faces the oncoming wind, HAWTs are highly efficient, capable of significant energy production, and are widely used. Alternatively, Vertical Axis Wind Turbines (VAWTs) have a vertical axis—perpendicular to the ground—and can face any direction. Since the critical components of VAWTs are located at their base, maintenance is simplified, ensuring ease of repairability. The disadvantages however are that VAWTs are not as efficient and are prone to fatigue due to the variation in forces that are applied to them.

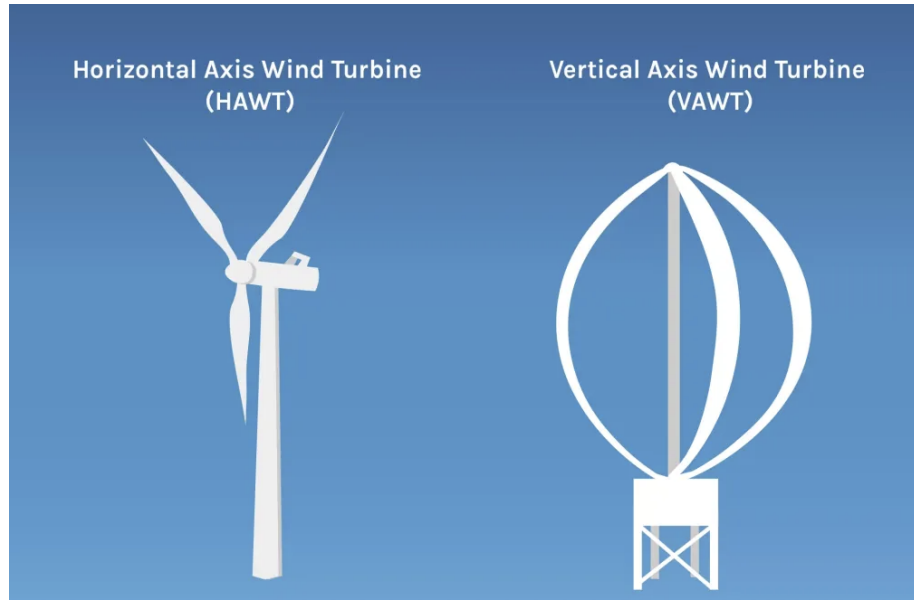


Figure 2: Diagrams of HAWT and VAWT Designs

Our project was to design, fabricate, and assemble a creative 3D-printed wind turbine, driven by the goal of maximizing both power output and stiffness. The design of our rotor was guided by four key parameters: the number of blades, blade profile, angle of twist, and angle of attack. Our team independently researched the optimal values of each and convened to produce a final blade design.

To meet the requirements of our project, we worked within constraints, both regarding the material and geometry of our tower. We were provided with a 12x12x0.375 inch ABS platform, on which our tower was glued. Additionally, the tower's height was restricted, as the center of our motor shaft had to be 16 inches above the platform. One of the primary challenges our team faced was adhering to the project constraints, particularly the limitation on the tower's volume, which could not exceed 17 cubic inches.

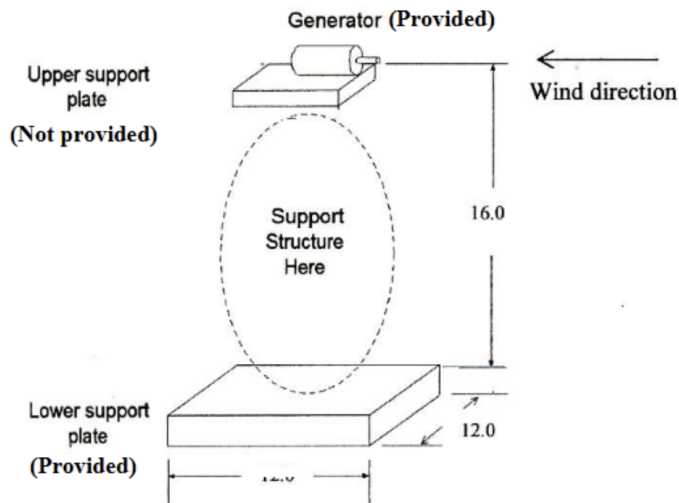


Figure 3: Diagram detailing the constraints and specifications of our wind turbine design

During our design process, we also included a housing for the provided motor, enabling measurements with a potentiometer. Beyond simply matching the dimensions of our motor, we also included a 3/16-inch hole aligned with the shaft to attach an eyebolt (to hang weights during deflection testing). Although given the CAD file for our rotor's hub, we designed the blade geometry, while remaining within a 3-inch radius from the central axis, based on provided constraints.

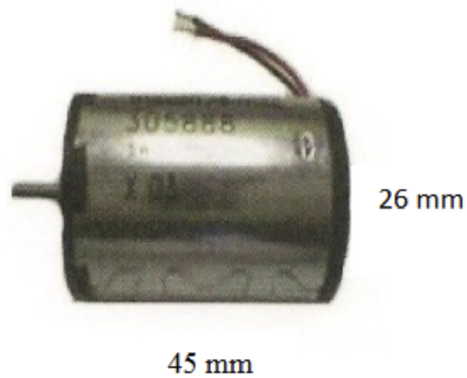


Figure 4: Motor Used for Testing

All parts for this project were printed using a 3D printer with a build volume of 9 x 9 x 9 inches. To fit within this size, our tower had to be printed as two separate parts which would then be glued together. Our tower also had to be radially symmetric and with a large contact

surface for gluing to the base. During this project, we opted to print our own parts to gain experience with operating a 3D printer.

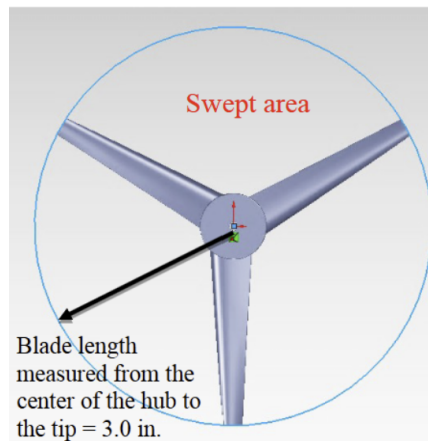


Figure 5: Diagram of rotor

Based on information provided by Professor Youssefi during lectures, coupled with our own independent research during Lab 5, we ultimately narrowed the design of our rotor. Namely, this required determining quantitative values for key parameters, including the number of blades, angle of attack, blade profile, and twist angle. According to a study conducted by Adeyeye et al, a wind turbine ought to use the minimum number of blades necessary to produce the desired performance. Namely, through the lens of cost-benefit analysis, adding on additional blades symbolizes a diminishing return, with increasing costs but little gain in energy production. Thus, to determine the ideal quantity of blades, we began at the minimum and increased the blade count until a stable configuration was found. The cases of zero and one blade are clearly impractical, as the former produces no rotary motion and the latter is imbalanced. Thus, we moved to two blades. Although seemingly practical, past work by Ikeda et al. found this setup conducive to unstable vibrations. Ultimately, therefore, our analysis converges at 3 blades, which offers a balanced and stable model for the wind turbine. While researching the angle of attack, our group unanimously agreed on ~7 degrees, supported by a wealth of existing literature. During research, we also found significant support for a high angle of twist, of upwards of 20 degrees. However, implementing this in practice proved challenging, as we found ourselves limited by the thickness of the provided hub; this shortcoming is addressed below. While researching airfoil geometries, we considered a number of options, including the NREL series and convex geometries, but ultimately decided to pursue the NACA 4412 profile, as seen below. This decision was guided by the limitations of our fabrication technique. As FDM printers struggle with thin tapers, we opted for a comparatively thick airfoil to ensure rigidity under high wind speeds.

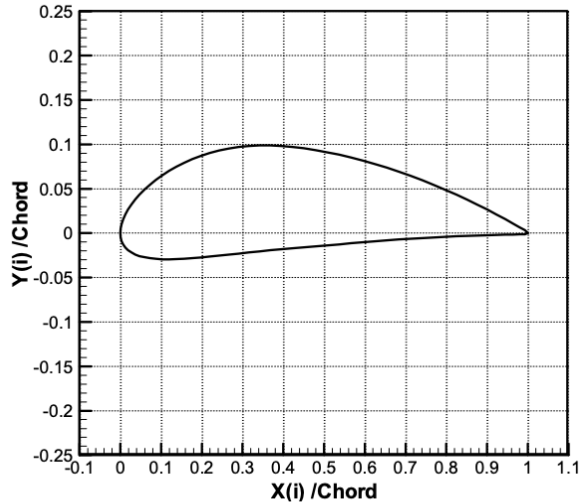


Figure 3. NACA 4412 airfoil profile.

Figure 6: The NACA 4412 airfoil we chose to utilize in our design.

DESIGN

Design Software:

To design the parts featured in this project, our team opted to use Solidworks, a 3D CAD design software with support for finite element analysis through Solidworks Simulation and rendering through Solidworks Visualize. Solidworks utilizes parametric-based design, enabling users to easily define complex geometries, such as a wind turbine rotor and tower. Workflows in Solidworks can be discretized into individual features, which, when combined in sequence, can be used to produce a desired final shape. These features include simple commands, such as Extrude and Revolve, which convert a two-dimensional sketch into a 3D volume and more complex tools, such as the Sweep and Loft, which enable the creation of more complex designs.

Turbine Design:

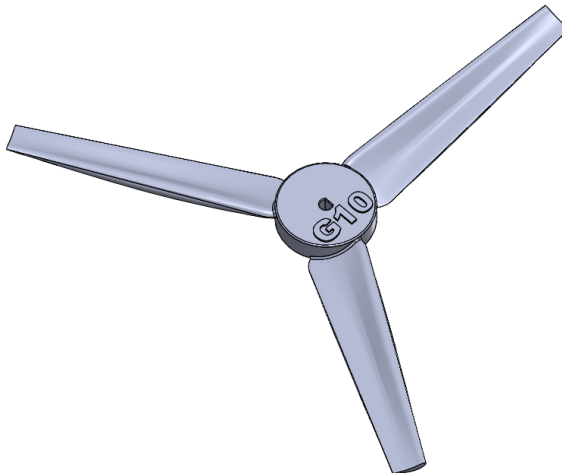


Figure 7: An isometric view of our completed rotor.

Following thorough research by all team members (see previous section), we ultimately opted to pursue a 3 rotor design, aiming for an approximate angle of attack 6-8 degrees, an angle of twist of 15 degrees, and a blade profile loosely inspired by the NACA 4412. To remain within the provided constraints while maximizing the swept area of our blade—and therefore maximizing power generation—we designed the rotor with a diameter of 5.9in.

To implement this geometry in CAD, we began with the provided hub and sketched three airfoil profiles to join via a loft. In addition, we added guide curves for the edges of the airfoil to ensure the lofted geometry did not exceed the width of the hub. Airfoil shapes were traced using a sketch image of the NACA 4412 airfoil with spline geometry to accurately capture the desired profile. Using the circular pattern tool, this blade was propagated around the hub. Finally, using the text tool, we added the “G10” characters to the face of the rotor.

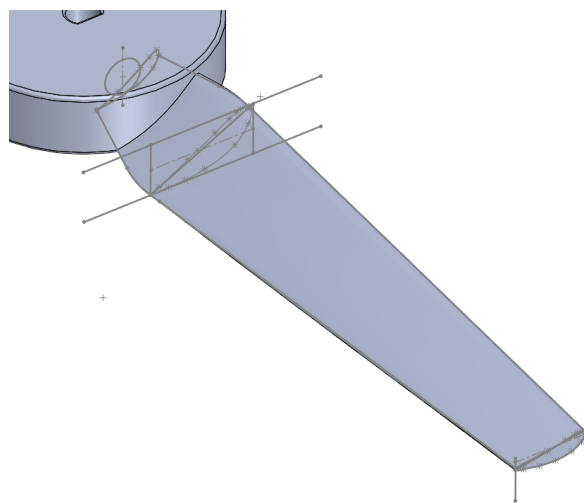


Figure 8: The three cross-sectional sketches and accompanying guide curves.

Tower Design:

To guide the design of our tower, we began with initial brainstorming through sketches, grounded in fundamental geometric principles—such as the importance of triangular cross-bracing. More specifically, team members individually drew the structures seen below, amongst others, which served as a guiding baseline for our CAD.

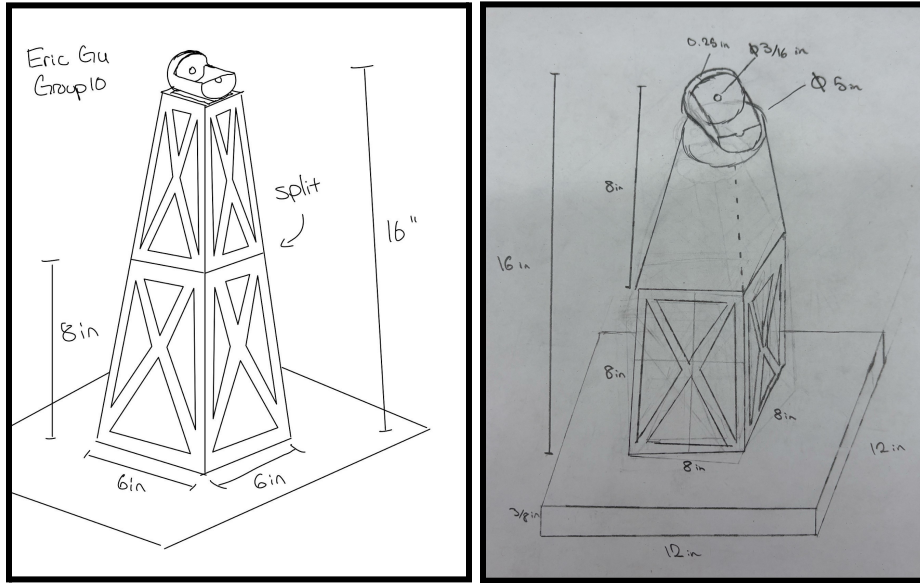


Figure 9: Initial tower illustrations by Eric Gu and Kavish Kondap, featuring cross-bracing for stability.

Wanting to pursue a geometry that not only was structurally sound but also utilized more complex Solidworks features, such as sweeps and lofts, our initial prototypes in Solidworks utilized similar structural members to the above sketches, but with more curvilinear geometry. The narrow base of our first concept lacked structural integrity and would lead to significant deflection under load, thus inspiring the second, tapered design, seen on the right below.

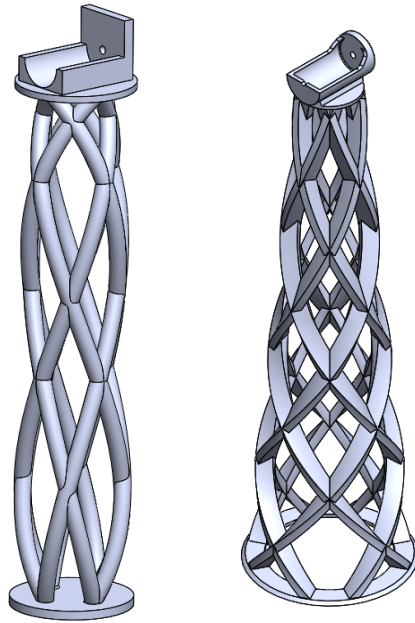


Figure 10: Initial tower design concepts in Solidworks. The right geometry was eventually converted into our final tower.

Realizing the stability of a triangular base, we later pivoted our design to include a more rigid lower half and used Solidworks' Loft feature to transition from a triangular to a circular cross-section. Including fillets between the intersecting spirals improved the rigidity of our design. To convert our monolithic structure into two parts, we utilized a Split feature and added tapered male and female pegs to ensure an easy-to-align connection when 3D printed. The parts were joined using Loctite 435 ABS Glue.

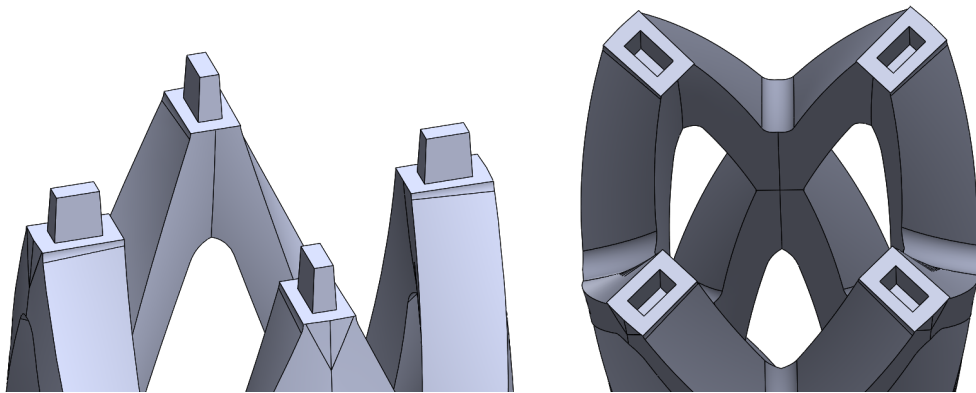


Figure 11: The pegs created on the bottom and top pieces (left and right) for simple alignment

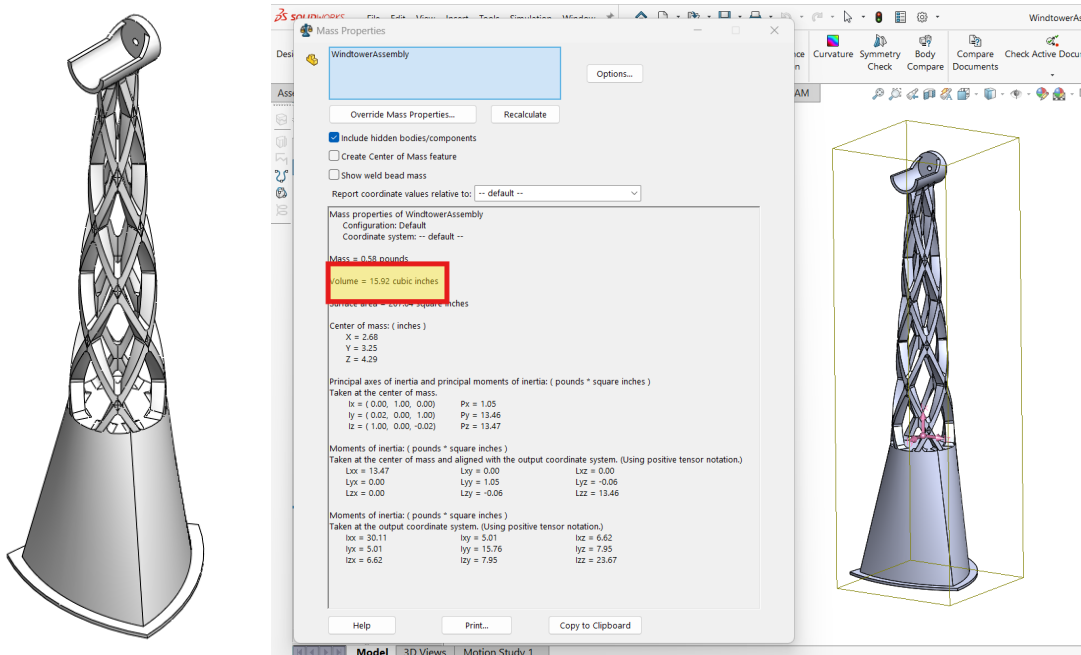


Figure 12: Our completed tower and a screenshot of the Solidworks properties window, showing a volume of 15.92 in^3

As seen above, our final tower design has a volume of 15.92 in^3 , which falls under the 17 in^3 limit for this project. This design also adheres to the project specifications listed below:

- A $\frac{3}{16} \text{ in}$ hole in line with the motor shaft is present to fasten the eyebolt during testing
- Our tower is made from two parts, each with a footprint of less than $9 \times 9 \times 9 \text{ inches}$
- The tower is radially symmetric and has a large contact area

Finite Element Analysis:

To evaluate the rigidity of our tower design prior to physical construction, we leveraged Finite Element Analysis (FEA) to simulate expected loads during testing. To simplify the meshing process, the two pieces of the tower were combined into one part and thus were assumed to be fixed together. To minimize computational overhead while maintaining accuracy, the mesh for the tower's base was coarsified—an option made possible due to its simple geometry and large distance from the load. The resulting high-fidelity mesh contained 99,774 elements, ranging in size from $\sim 0.024\text{in}$ to $\sim 0.49\text{in}$. The high percentage of finite elements with aspect ratio < 3 (94.3%) implies a well-meshed geometry, as larger aspect ratios correlate to inaccurate measurements during simulation. A fixture was applied to the base of the tower, representing the glued attachment to the baseplate, and a 9.8N tension load was applied to the motor housing, simulating the presence of a 1kg weight, identical to the experiment we plan on running during testing.

Mesh Details	
Study name	Static 1 (-Default-)
DetailsMesh type	Solid Mesh
Mesher Used	Blended curvature-based mesh
Jacobian points for High quality mesh	16 points
Max Element Size	0.488233 in
Min Element Size	0.0244116 in
Mesh quality	High
Total nodes	162053
Total elements	99774
Maximum Aspect Ratio	88.450
Percentage of elements with Aspect Ratio < 3	94.3
Percentage of elements with Aspect Ratio > 10	1.26
Percentage of distorted elements	0.00401
Number of distorted elements	4
Reuse mesh for identical bodies	Off
Number of bodies that have reused mesh	0
Time to complete mesh(hh:mm:ss)	00:00:50
Computer name	KAVISH

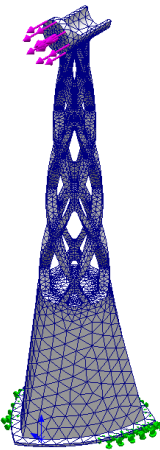


Figure 13: The mesh and accompanying details for a finite element analysis of our tower. A fixture on the base of the tower and a 9.8N load near the top can also be seen in green and pink, respectively.

After meshing and running the simulation with the aforementioned fixtures and load, we present the following plots of von Mises stress, displacement, and factor of safety:

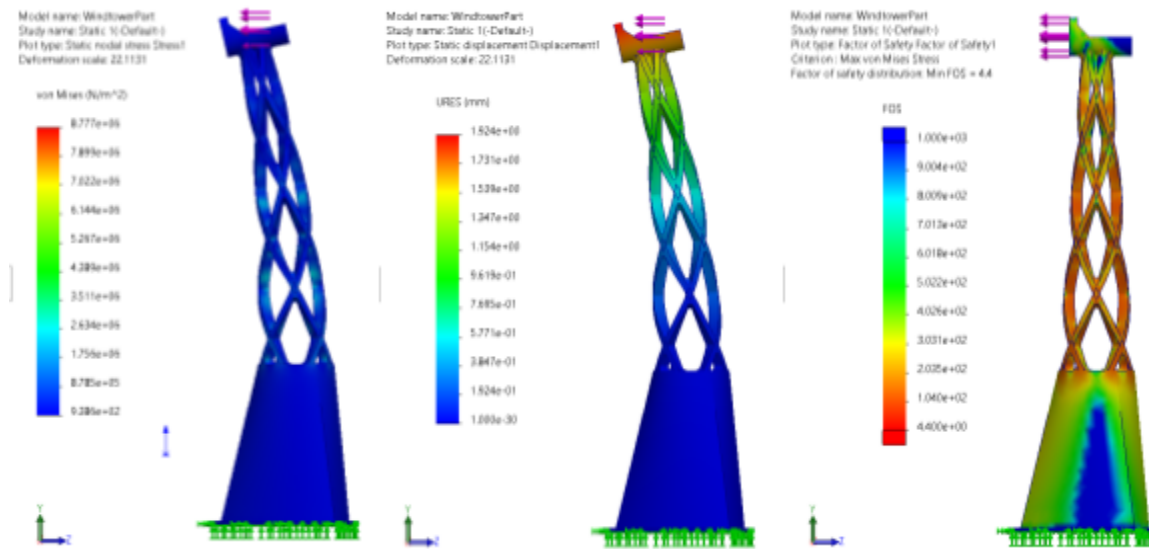


Figure 14: From left to right, plots of the von Mises stress, displacement, and factor of safety for our wind tower. For the stress and displacement plots, note the deformation scale of 22.131.

Based on the von Mises stress plot, the maximum stress given a 9.8N load is 8,777,000 N/m², which is significantly below the yield strength of ABS (20,000,000 N/m²). Thus, we can assume that the tower will not undergo plastic deformation in real life. When analyzing the deflection plot, we observe that the maximum deflection of the tower is around 1.924mm. An experiment measuring deflection with respect to applied load using FEA was also conducted; these results are shown in the next section and are compared to empirical measurements.

Finally, interpreting the factor of safety plot reveals a minimum FOS of 4.4, implying that the tower will remain standing under a load of $9.8N \cdot 4.4 = 43.12N$, which is equivalent to a 4.4 kg weight. As expected, the limiting factor determining the minimum FOS is the spiraling ribbons, which are more vulnerable to deflection than the dense triangular base.

TESTING AND RESULTS

Equipment and Instrumentation



Figures 15-20: The instrumentation used during testing. From left to right, top to bottom: Neiko Digital Tachometer, Kestrel Digital Anemometer, Mighty Mini Air Blower, Fowler Electronic Depth Gauge, Mettler Digital Scale, Potentiometer

During testing, we relied on the provided instrumentation to ensure an accurate and quantitative evaluation of our wind turbine's power generation and deflection. To measure the wind speed produced by our air blower, we used a digital anemometer. We used a digital tachometer to measure the tip speed of the blade in RPM. To measure the voltage, current, and power generated as a result of the motor on the tower, we used a potentiometer. To measure the

deflection of the tower itself, we utilized a depth gauge to measure our tower's bending to a high degree of precision. Finally, we used a digital scale to determine the mass of the tower.

Power Generation Test:

The first test we conducted was measuring the power output of the tower. To begin, we secured our wind turbine to the testing platform and positioned it directly in front of the air blower. Using a plastic zip tie, we fastened our motor into its 3D-printed housing and set the air blower to the maximum wind setting, which the anemometer measured to be 25 mph. Before we began collecting data points, we tested both sides of our rotor blade to determine which would produce more power and found that one of our sides produced no spin. Using the other side, we began our testing procedure. To allocate workload, we had team members manage the tachometer, potentiometer, and data transcription, while others took photos to document our process. When collecting data, we realized our power ranged between 100 and 500 watts, causing us to increment our data points by 30-40 ohms to ensure a wide range of values. We additionally chose to measure the power at resistances above our peak power to ensure we had reached the max. For each of the 15 data points, we recorded voltage, current, power, and the blade rotation speed as shown in the table below.

Data Points	Voltage (V)	Current (mAmp)	Power (mWatt)	Blade Rotational Speed (rpm)
1	2.35	44	105	3460
2	2.32	59	137	3455
3	2.26	78.4	175	3405
4	2.20	95	206	3366
5	2.15	107	235	3302
6	2.08	133	280	3240
7	2.02	157	315	3201
8	1.96	180	350	3123
9	1.91	193	370	3095
10	1.83	215	405	3018
11	1.69	265	450	2883
12	1.45	335	500	2683
13	1.31	370	475	2522
14	1.16	383	440	2354
15	1.00	415	405	2126
16	0.72	425	290	1733

Table 1: Potentiometer and tachometer data from rotor testing.

Based on the data in table 1, we observe that the max power output from our rotor is 0.5W, corresponding with potentiometer readings of 1.45V, 335mA, and an RPM of 2683 RPM.

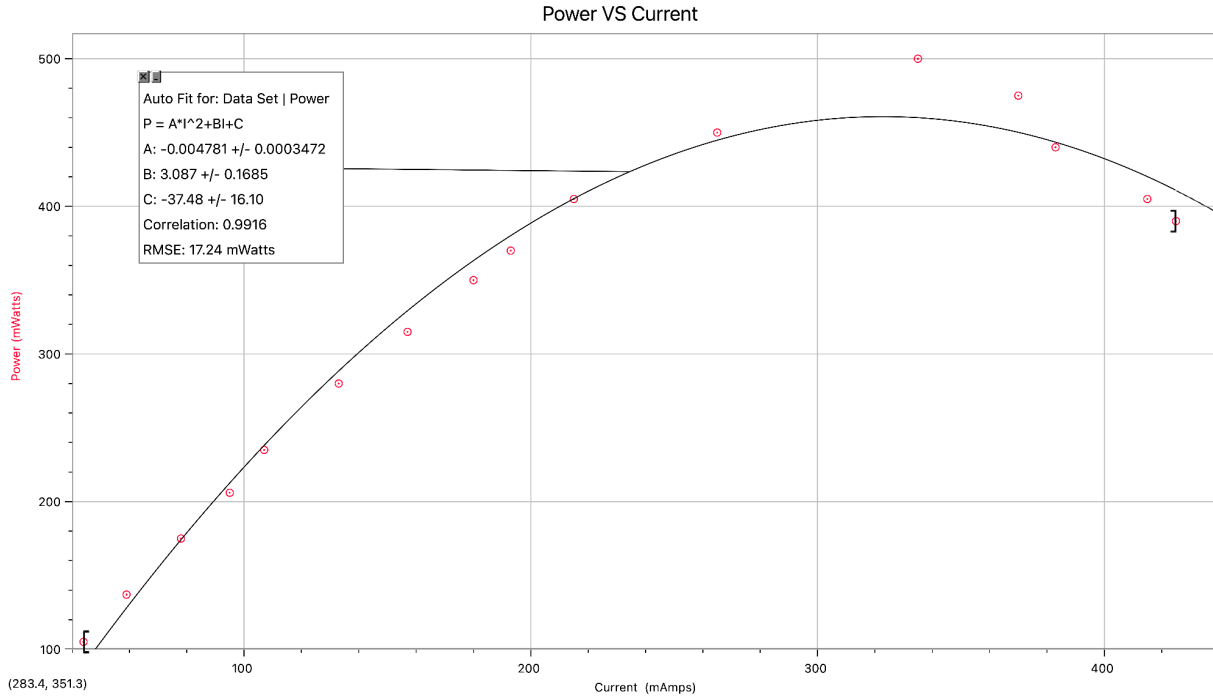


Figure 21: Graph of Current vs Power

Applying a curve to the data, we found a parabola to be the best fit for the above graph. This shows that as the current is increased, the power increases to a maximum of 0.5 watts, before decreasing. This illustrates the challenge in optimizing power, as it is not simply a linear increase proportional to current, but instead, a specific maximum which had to be found by varying the resistance of the potentiometer.

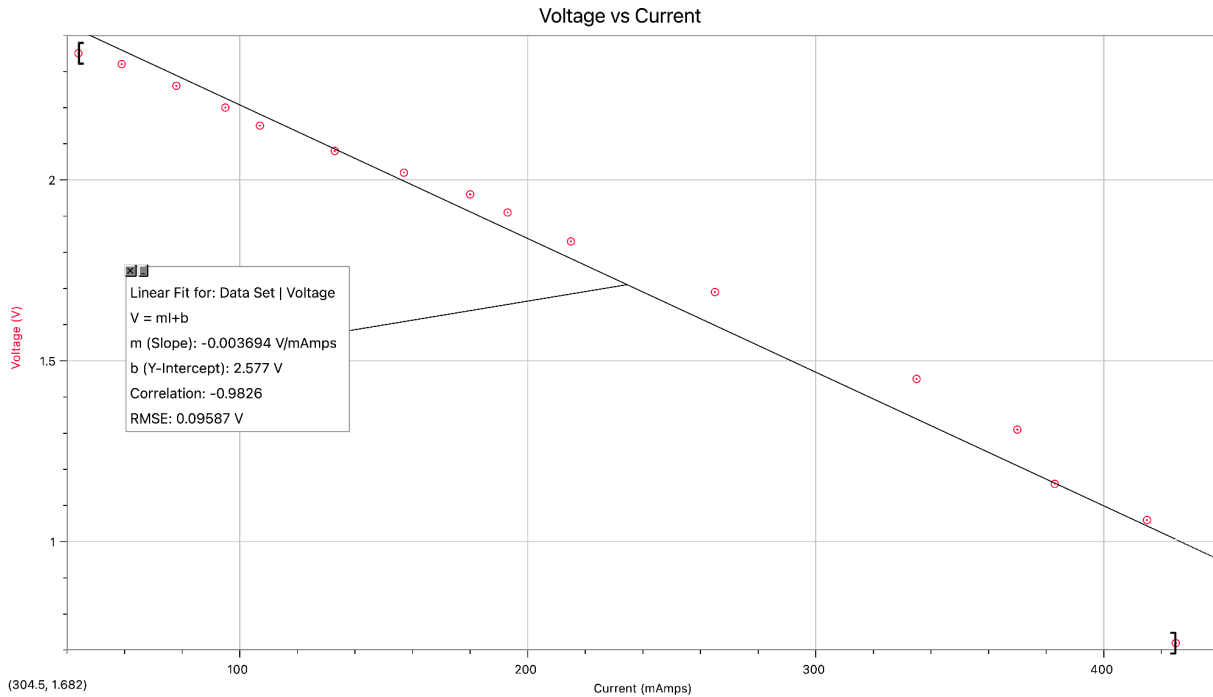


Figure 22: Graph of Current vs Voltage

The above graph shows an inverse linear relationship between current and voltage. As the current was increased, the potentiometer showed that the voltage decreased proportionally. The correlation factor R^2 is 0.9604, showing the observed trend is due to the inverse linear relationship between current and voltage, as well as the fact that the data is accurate.

To compute the efficiency of our wind turbine, we follow the formula

$$\text{efficiency} = \frac{\text{experimental power}}{\text{theoretical power}} \cdot 100$$

From the above charts, we see that our experimental power is 0.5 Watts. To calculate the theoretical power, we utilize the known speed of the moving air to determine power. Since power is defined as the change in kinetic energy over time, we can think of this calculation as the following formula:

$$P = \frac{1}{2}mv$$

Where m is the mass per second passing through the cross-section of our rotor. Substituting relevant variables yields:

$$P = \frac{1}{2} [\rho Av]v^2 = \frac{1}{2}\rho\pi r^2 v^3$$

Where ρ is the density of air (1.225 kg/m^3) r is the radius of our rotor (150mm) and v is the wind velocity (25 mph, or 11.176 m/s). Plugging in numeric values leads to a theoretical max power of 60.44 W. Thus calculating for efficiency, we get 0.83%. Comparing this to the theoretical maximum value specified by the Betz Limit (59.3%) and the efficiency of modern-day wind turbines (20-40%), we notice that our 3D-printed project has room for improvement. Much of our inefficiency likely stems from a lack of computational optimization for the airfoil geometry, as is

common in industry. Combined with more iterative testing, these techniques would result in a more efficient rotor.

Deflection Testing:

The second test we conducted was a deflection test. We began by aligning our tower to the pulley system and clamped the structure to a workbench. We then attached a string to the eyebolt so the weight could be added on the other side. By taping a spacer into our motor housing, we ensured consistent measurements from our depth gauge. After zeroing the system, we added weight in 100 g increments and measured the deflection each time.

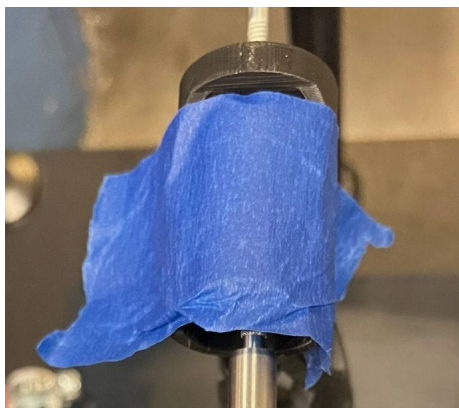


Figure 23: The spacer taped into our motor housing

In total, we collected 14 data points, including the initial null measurement. For the first 11 data points, we recorded the displacement while adding the weight in 100g increments in mass, until 1 kg was reached. For the 3 final data points, we experimented with higher increments of weight to measure the stiffness of the tower to see if it fails. As these measurements fall outside project guidelines, they are not included in our following analysis and calculations. Although the gauge neared its physical limit, we successfully measured the deflection of our tower when loaded with 3.5 kg.

Data Points	Load (g)	Displacement (mm)	Observation
1	0	0	No visible Deflection
2	100	0.15	No visible Deflection
3	200	0.45	No visible Deflection
4	300	0.75	No visible Deflection
5	400	1.02	No visible Deflection
6	500	1.29	No visible Deflection
7	600	1.58	No visible Deflection
8	700	1.86	No visible Deflection
9	800	2.12	No visible Deflection
10	900	2.39	No visible Deflection
11	1000	2.63	No visible Deflection
<i>Measurements with additional weight</i>			
12	2000	5.38	No visible Deflection
13	3000	8.37	No visible Deflection
14	3500	9.63	No visible Deflection

Table 2: Measurements from our deflection experiment

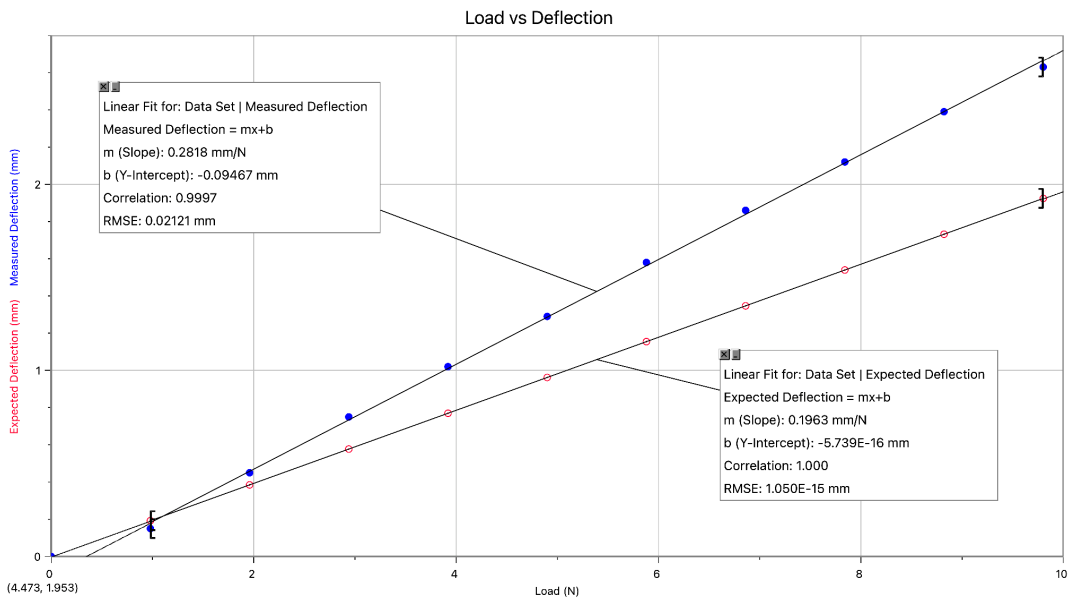


Figure 24: Graph of Load vs Deflection

The above graph compares both the measured and expected deflection, which was calculated using FEA, against the load (see previous section). The R^2 value for our measured data is 0.994, while the simulated data follows a perfectly linear trend ($R^2=1.000$). As shown in the graph, the measured deflection (2.63mm) is noticeably higher than the expected deflection (1.92mm). This discrepancy is explained in later sections. Stiffness can then be calculated through the following equation:

$$\text{Stiffness} = \frac{\text{Load}}{\text{Deflection}}$$

Realizing that this is the inverse of the slopes of the above graph, we find that the measured stiffness is $3.55 \frac{N}{mm}$ and the expected stiffness is $5.09 \frac{N}{mm}$, showing that the tower is significantly less stiff in practice than expected. Calculating the stiffness-per-gram ratio follows the following formula:

$$\frac{\text{stiffness}}{\text{net weight (kg)}} = \frac{3.55}{0.178} = 19.9 \frac{N}{mm \cdot kg}$$

CAD DRAWINGS

Figure 25: Renders of the wind turbine and exploded view.

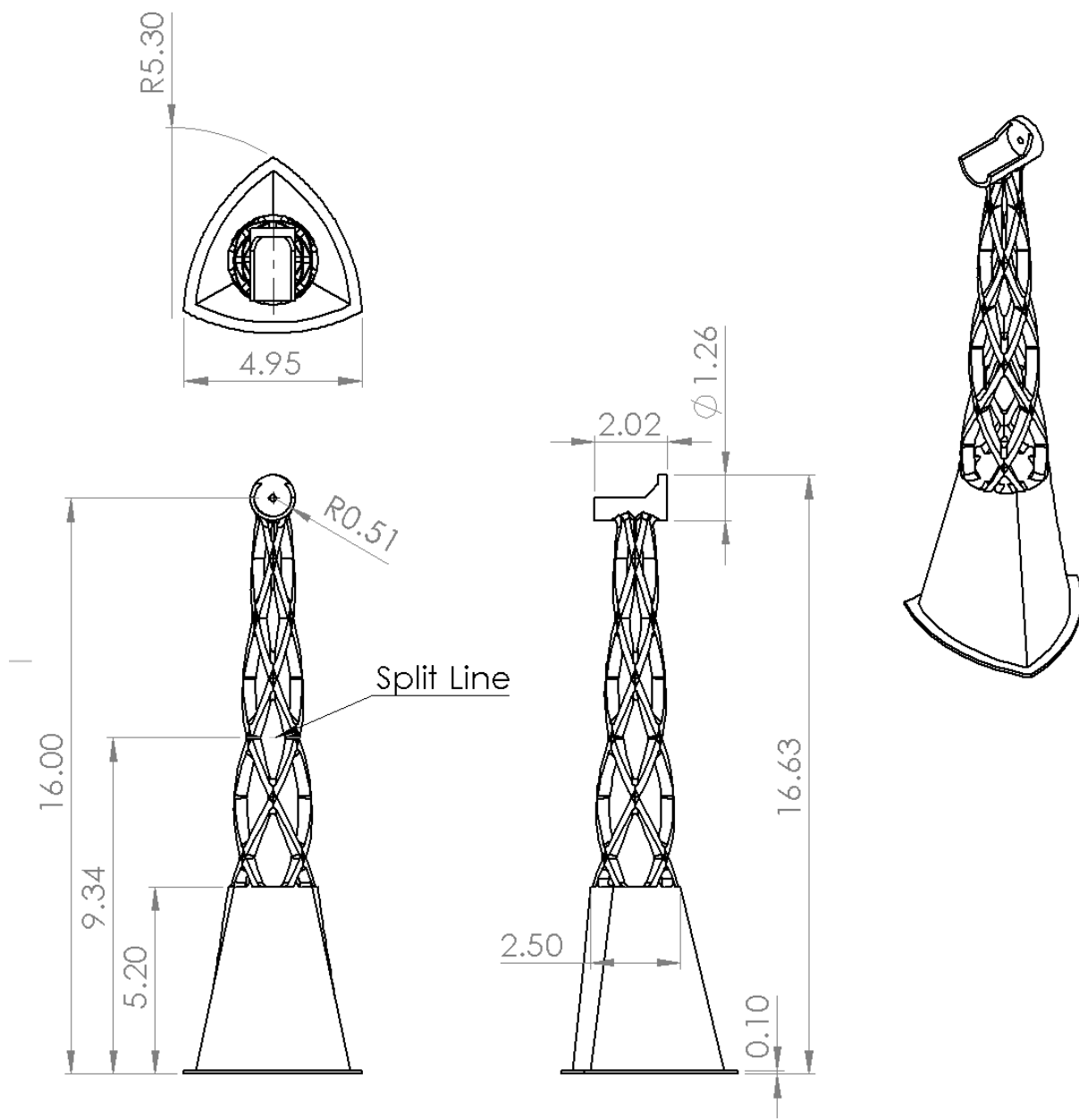


Figure 26: Drawings of the tower.

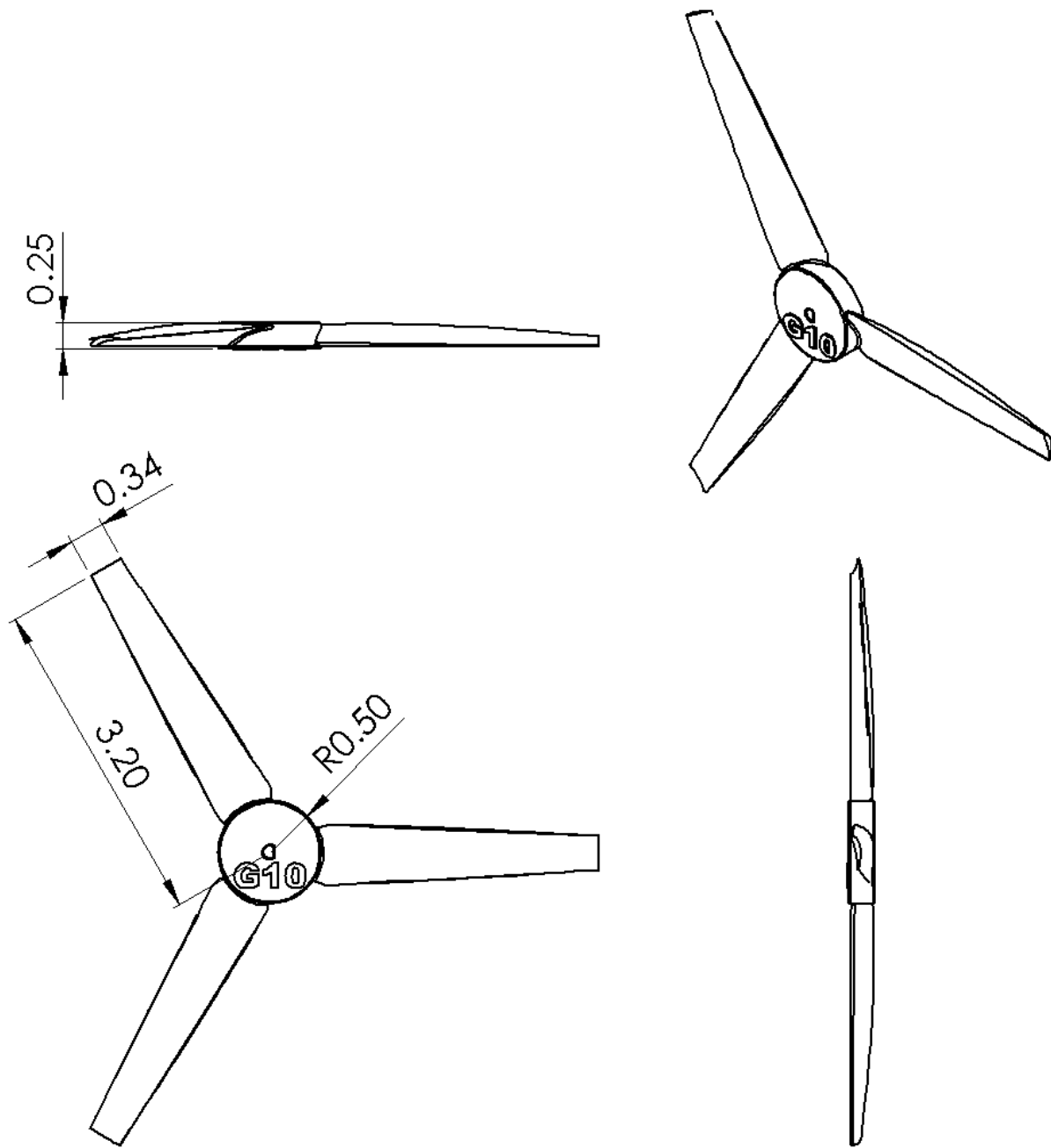


Figure 27: Drawing of the rotor.

CONCLUSION

Through this project, we gained valuable insights into the wind turbine design process and its real-world performance. We conducted extensive research, leveraging publicly available data and studies to inform our design. This process taught us about critical factors such as twist, angle of attack, and the number of blades of an airfoil. We then created a CAD model of the turbine, 3D-printed it, and subjected it to tests for power generation and deflection resistance.

During the deflection test, we observed a significantly larger displacement than predicted by our Solidworks FEA simulations. Namely, despite expecting a flex of under 2mm, our empirical testing yielded 25% higher-than-anticipated deflection. This may have been due to the presence of ~5% of the mesh elements in FEA with an excessively large aspect ratio and could be resolved with a finer mesh and more computing power. Additionally, FEA is limited by fundamental simplifications, such as assuming the material to be isotropic. Since 3D printing is inherently done in layers, this is not true in real life, and since the layer lines of our tower aligned with the direction of applied force, it is possible that this caused more deflection.

Although matching the expected linear trend between voltage and current and the parabolic relationship between power and current, our power output was lower than anticipated, with only a quarter of the desired 2W output. Despite these challenges, the project provided us with a deeper understanding of the limitations of FEA simulations and the impact of real-world variables. We also identified design improvements that could be implemented to achieve better outcomes in future iterations.

RECOMMENDATIONS FOR FUTURE WORK

Our empirical results from testing proved to be highly insightful and would be invaluable in guiding a future iteration of the wind turbine and rotor design.

Rotor Improvements:

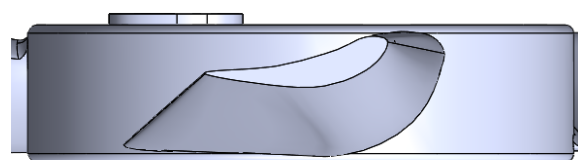


Figure 28: A side profile view of the rotor, showing a lack of twist

Upon further review of our rotor, we noticed that, despite attempting to include a large angle of twist, due to the thickness constraints imposed by the provided hub, our empirical twist was minimal, resulting in a nonoptimal design. Put simply, due to the lack of twist, the edges of our rotor contributed little to producing rotary force. Attempting to include more twist, while

adhering to the constraints of the hub's thickness would have enabled more air hitting the blades to be converted into rotational motion. Additionally, during testing, we observed that one side of our existing rotor was "dead", according to Professor Youssefi, implying it was unable to produce a lift vector. This corresponds with our observations of a lack of twist.

Tower Improvements:

Following the deflection test, it became apparent that a wider tower base would have led to less deflection, despite needing thinner structural members to fit within the volume constraints. By spreading the load over a larger area, the tower's flex would be minimized, therefore maximizing stiffness. Additionally, once 3D printed with a lighter infill, our tower weighed merely 178g, far below the limit of this project. By simply increasing the thickness of the existing structure, we would have achieved less deflection and more rigidity.

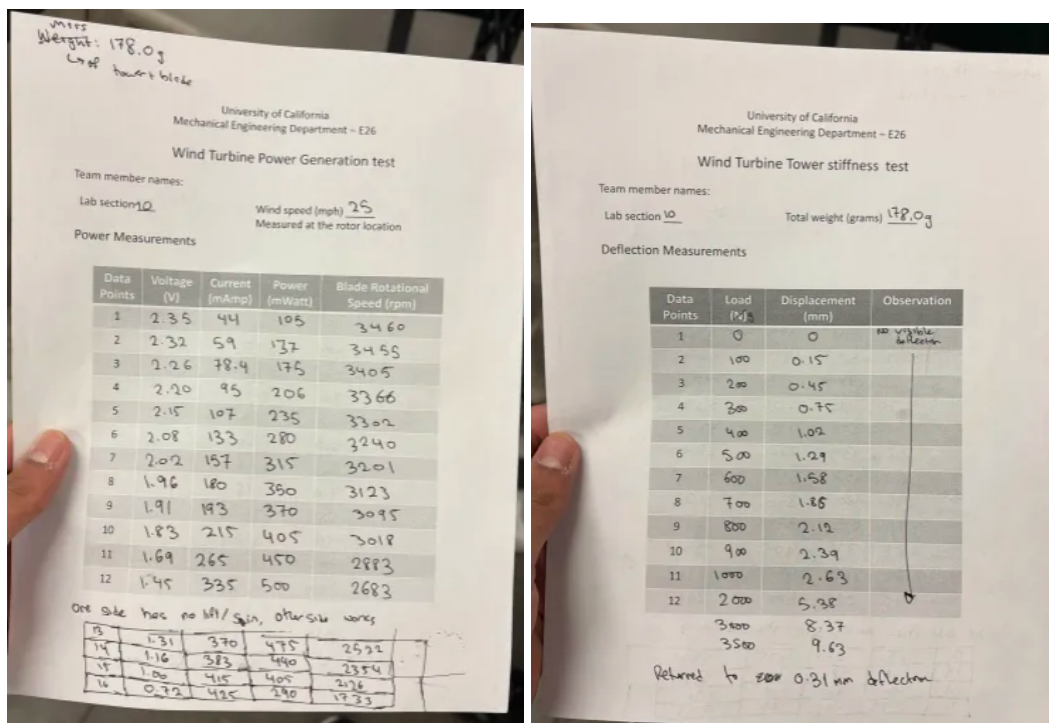
REFERENCES

1. Acrylonitrile Butadiene Styrene (ABS Plastic): *Uses, Properties & Structure*. (2019). Omnexus. <https://omnexus.specialchem.com/selection-guide/acrylonitrile-butadiene-styrene-abs-plastic>
2. Adeyeye, K. A., Ijumba, N., & Colton, J. (2021). The Effect of the Number of Blades on the Efficiency of A Wind Turbine. *IOP Conference Series: Earth and Environmental Science*, 801(1), 012020. <https://doi.org/10.1088/1755-1315/801/1/012020>
3. *Betz Limit and a Wind Turbines Coefficient of Power*. (n.d.). Alternative Energy Tutorials. <https://www.alternative-energy-tutorials.com/wind-energy/betz-limit.html>
4. Energy Education. (2018). *Betz limit - Energy Education*. Energyeducation.ca. https://energyeducation.ca/encyclopedia/Betz_limit
5. Youssefi, Ken. *Wind Turbine Aerodynamics*. October 10, 2024, Engineering 26, University of California, Berkeley. Powerpoint Slides.
6. Youssefi, Ken. *Wind Turbine Project Description*. 2024. Engineering 26, University of California, Berkeley. Document.
7. *MatWeb - The Online Materials Information Resource*. (n.d.). [Www.matweb.com](http://www.matweb.com). <https://www.matweb.com/search/DataSheet.aspx?MatGUID=3a8afcddac864d4b8f58d40570d2e5aa&ckck=1>
8. National Grid. (2024, April 24). *The history of wind energy | National Grid Group*. [Www.nationalgrid.com](http://www.nationalgrid.com). <https://www.nationalgrid.com/stories/energy-explained/history-wind-energy>
9. NREL. (2019). *Wind Energy Basics | NREL*. [Nrel.gov](http://www.nrel.gov). <https://www.nrel.gov/research/re-wind.html>
10. Sofia. (2022, July 17). *What is a Wind Turbine?* Lindy Energy. <https://lindyenergy.com/what-is-a-wind-turbine/>
11. University of Michigan. (2021). *Wind Energy Factsheet*. Center for Sustainable Systems. <https://css.umich.edu/publications/factsheets/energy/wind-energy-factsheet>

12. Wind Energy Technologies Office. (n.d.). *Advantages and Challenges of Wind Energy*. Energy.gov; Office of Energy Efficiency & Renewable Energy.
<https://www.energy.gov/eere/wind/advantages-and-challenges-wind-energy>
13. Wind Energy Technologies Office. (2024). *How Do Wind Turbines Work?* Office of Energy Efficiency and Renewable Energy; U.S. Department of Energy.
<https://www.energy.gov/eere/wind/how-do-wind-turbines-work>

APPENDICES

Appendix A: Additional Media



The image contains two side-by-side photographs of handwritten data tables.

Left Photograph (Wind Turbine Power Generation test):

Handwritten notes at the top left:
 Wind speed: 25 mph
 Measured at the rotor location
 Lab section 10
 Total weight (grams) 178.0g
 Date: 10/10/24

Table header: University of California Mechanical Engineering Department - E26
 Wind Turbine Power Generation test
 Team member names:
 Lab section 10 Wind speed (mph) 25
 Measured at the rotor location

Power Measurements

Data Points	Voltage (V)	Current (mAmp)	Power (mWatt)	Blade Rotational Speed (rpm)
1	2.35	44	105	3460
2	2.32	59	137	3455
3	2.26	78.4	175	3405
4	2.20	95	206	3366
5	2.15	107	235	3302
6	2.08	133	280	3240
7	2.02	157	315	3201
8	1.96	180	360	3123
9	1.91	193	370	3095
10	1.83	215	405	3018
11	1.69	265	450	2883
12	1.45	335	500	2683

One side has no lift/spin, otherwise works

13	1.31	370	495	2522
14	1.16	383	440	2354
15	1.05	415	405	2126
16	0.72	425	290	1933

Right Photograph (Wind Turbine Tower stiffness test):

Handwritten notes at the top right:
 Wind speed (mph) 25
 Measured at the rotor location
 Lab section 10 Total weight (grams) 178.0g
 Date: 10/10/24

Table header: University of California Mechanical Engineering Department - E26
 Wind Turbine Tower stiffness test
 Team member names:
 Lab section 10 Total weight (grams) 178.0g

Deflection Measurements

Data Points	Load (kg)	Displacement (mm)	Observation
1	0	0	No visible deflection
2	100	0.15	
3	200	0.45	
4	300	0.75	
5	400	1.02	
6	500	1.29	
7	600	1.58	
8	700	1.85	
9	800	2.12	
10	900	2.39	
11	1000	2.63	
12	2000	5.38	
	3000	8.37	
	3500	9.63	

Returned to 2000 0.31 mm deflection

Figure 29: Raw Testing Data



Figures 30-31: Testing power generation (left) and deflection (right) setups, which may prove useful for replicating results.